MAY 27, 2020
CONFERENCE ONLINE

Graphene Industrial Forum &2DM 2020

2D Van der Waals Lateral Spin Valve

Aybey MOGULKOC[1], Yesim MOGULKOC[2], Mohsen MODARRESI[3] and Alexander RUDENKO[4,5,6]

[1]Faculty of Science, Department of Physics, Ankara University, Ankara, Turkey., [2]Faculty of Engineering, Department of Physics Engineering, Ankara University, Ankara, Turkey.
[3]Department of Physics, Ferdowsi University of Mashhad, Mashhad, Iran [4]School of Physics and Technology, Wuhan University, Wuhan 430072, China
[5]Radboud University, Institute for Molecules and Materials, Heyendaalseweg 135, 6525 AJ Nijmegen, Netherlands. [6]Theoretical Physics and Applied Mathematics Department, Ural Federal University, 620002 Ekaterinburg, Russia.

http://hymf.ankara.edu.tr

Motivation

- A spin-valve device usually consists of two ferromagnetic (FM) thin films separated by a nonmagnetic spacer. The electron-transport properties of such a device depend on the relative orientation of magnetization in the individual FM layers.
- For current passing perpendicular to the FM layers, the majority-spin states are conductive, while the minority-spin electrons are reflected or spin-flip scattered due to the lack of empty electronic states. As a result, if the magnetic alignment of magnetic layers is parallel, the total conductivity through the device is mostly determined by the spin-up channel.
- Spin valves have found application in information storage, logical devices, and magnetic sensors [1–9].
- With the emergence of two-dimensional (2D) materials, they are being proposed as building blocks for spin-valve devices. Recently, some vertical spin valves based on thin FM layers and 2D spacers were fabricated [1,10,12].
- Another milestone in the field was set by the discovery of 2D ferromagnets [12]. CrI_3 was the first magnetic 2D material, with a Curie temperature of 45 K [13].

Method

- The first-principles electronic structure calculations performed in this study are based on Density Functional Theory (DFT). The projected augmented-wave method [14,15] is used as implemented in the Vienna *ab initio* simulation package (VASP) [16,17].
- To capture the effects of strong electronic correlations, we use the DFT with Hubbard *U* parameter (DFT + *U*) method [18,19], applying the effective on-site Coulomb repulsion to the *d* orbitals of Cr atoms. Electronic transport properties are calculated within the semiclassical Boltzmann transport theory with use of the BOLTZWANN code [20] in conjunction with the WANNIER90 code [21] used to interpolate the band structure by means of the maximally localized Wannier functions [22,23].

Model

The interaction between the spins is modeled according to the classical Heisenberg Hamiltonian

$$H = \sum_{i,j} J_{ij}\,\mathbf{S}_i \cdot \mathbf{S}_j + \sum_i A_i(\mathbf{S}_i \cdot \mathbf{z}_i)^2,$$

where $J_{ij} \equiv J(\mathbf{R}_{ij})$ is the exchange interaction between spins $\mathbf{S}_i$ and $\mathbf{S}_j$, A_i is the single-ion anisotropy at spin $\mathbf{S}_i$, and $\mathbf{z}_i$ is the unit vector pointing in the direction of the easy-magnetization axis. To estimate the Curie temperature T_C for monolayer CrN and its heterostructures, the random-phase approximation [24] is considered within the Heisenberg Hamiltonian.

$$k_B T_C = \frac{2}{3}\frac{S+1}{S}\left(\frac{1}{\Omega}\int d\mathbf{q}\, N^{-1}(\mathbf{q})\right)^{-1}$$

where $\Omega = 8\pi^2/\sqrt{3}a^2$ is the Brillouin zone area and $N(\mathbf{q}) = +J(0) - J(\mathbf{q})$ is the spin-wave energy, with $J(\mathbf{q})$ being the Fourier transform of $J(\mathbf{R}_{ij})$, and $\Delta = AS^2$ is the magnetocrystalline anisotropy. By expanding the spin-wave energy up to the second order in *q*, we arrive at the following formula for the Curie temperature:

$$k_B T_C = \frac{8\pi\sqrt{3}}{3}\frac{S+1}{S}\frac{JS^2}{\ln\left[\frac{\Delta+4\pi\sqrt{3}JS^2}{\Delta}\right]}.$$

Goals of This Study

- We study the electronic, magnetic, and transport properties of a CrN based spin valve.
- We consider two hexagonal CrN monolayers separated by a blue-phosphorus insulating spacer, which is perfectly commensurate with the CrN structure.

Results

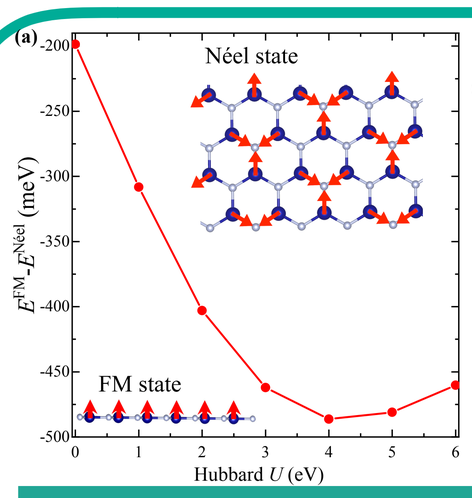

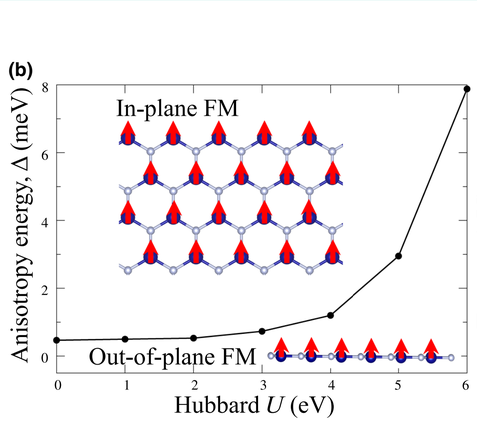

(a) Energy difference between the FM and Néel states in single-layer CrN calculated per Cr atom as a function of the Hubbard *U* parameter. (b) The magnetic anisotropy energy (Δ) calculated per Cr atom as the difference between the out-of-plane and in-plane FM configurations in single-layer CrN for a series of Hubbard *U* parameters. The insets show the alignment of spins for the different magnetic configurations.

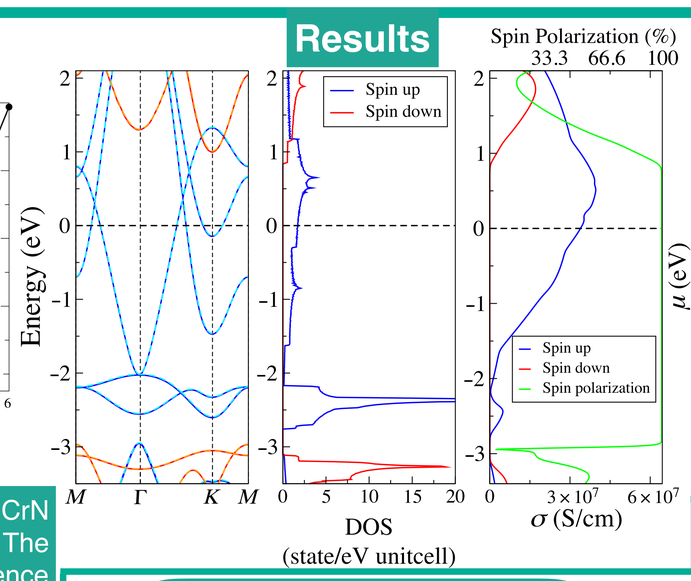

(a) Electronic bands calculated for spin-up (blue line) and spin-down (red line) states of monolayer CrN. The dashed lines are the DFT bands, while the solid lines are the Wannier interpolated bands. (b) The corresponding spin-resolved DOS. (c) Spin-up ($\sigma^{\uparrow}$) and spin-down ($\sigma^{\downarrow}$) components of the lateral conductivity, as well as its spin polarization calculated as a function of the chemical potential μ.

$$\sigma_{SP} = \frac{\sigma^{\uparrow} - \sigma^{\downarrow}}{\sigma^{\uparrow} + \sigma^{\downarrow}}.$$

For monolayer CrN, the spin polarization is 100% for any realistic doping regime, which indicates perfect spin filtering.

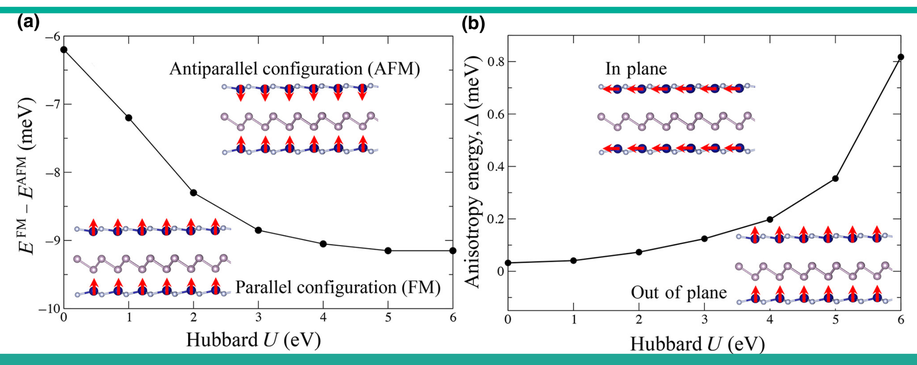

(a) Energy difference between parallel (FM) and antiparallel (AFM) configurations in CrN/P/CrN calculated per Cr atom depending on the Hubbard *U* values. The insets show the spin distribution for both configurations. (b) The anisotropy energy (= $E^{in} - E^{out}$) per Cr atom.

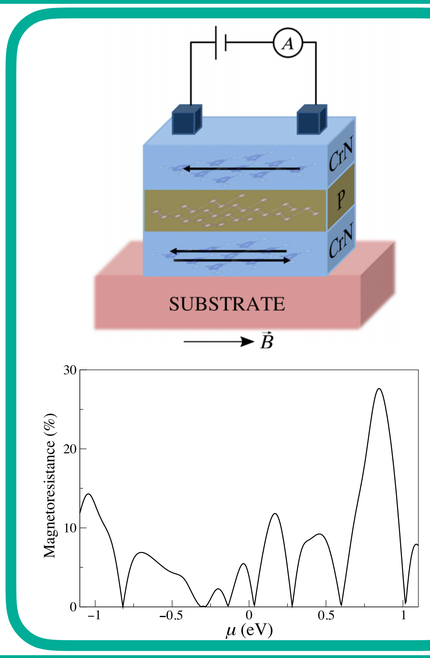

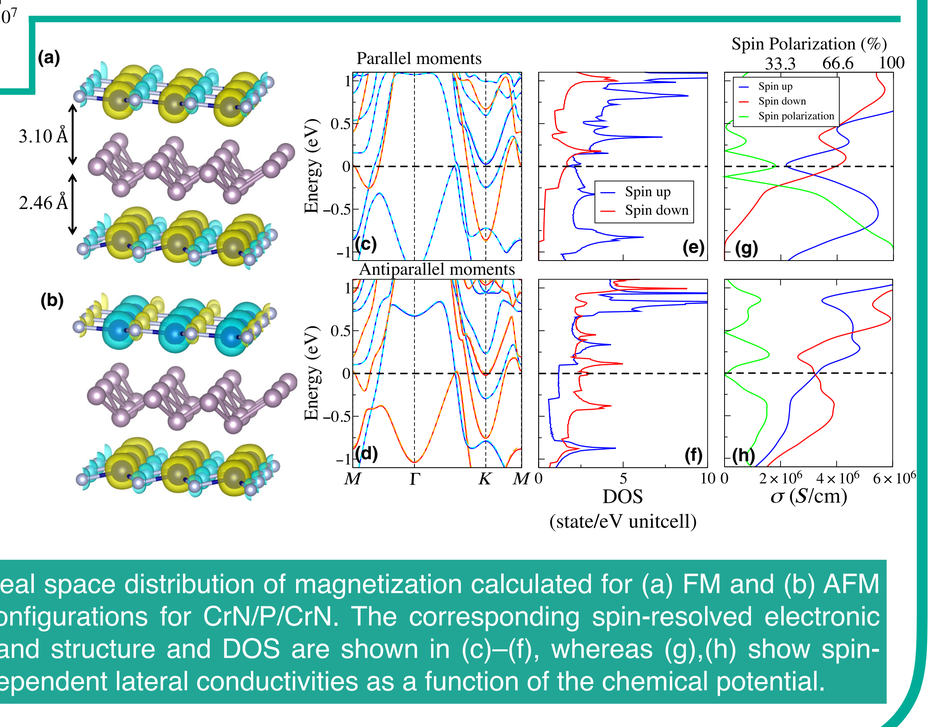

Real space distribution of magnetization calculated for (a) FM and (b) AFM configurations for CrN/P/CrN. The corresponding spin-resolved electronic band structure and DOS are shown in (c)–(f), whereas (g),(h) show spin-dependent lateral conductivities as a function of the chemical potential.

System	M (μ_B)	J (meV)	Δ (meV)	T_c (K)
CrN ($U = 0$ eV)	3.00	4.90	0.47	496
CrN ($U = 3$ eV)	3.00	11.41	0.73	1084
CrN/P	2.53	13.33	0.11	968
CrN/P/CrN	2.63*	12.29	0.12	910

*The value is given for FM configuration. In the AFM case, $M = 0.16\ \mu_B$.

Net magnetization per Cr atom (*M*), Heisenberg exchange interaction (*J*), on-site anisotropy energy (*Δ*), and the Curie temperature (T_c) estimated in this work for monolayer CrN, bilayer CrN/P, and trilayer CrN/P/CrN. The values for monolayer CrN are given for two different Hubbard U parameters. In other cases, U = 3 eV is assumed.

Conclusions

- We calculate the exchange interactions and single-ion anisotropy parameters to estimate the Curie temperature within the random-phase approximation, which is found to be around 910 K for CrN/P/CrN
- The calculated magnetoresistance is around 12% in the low-doping regime.
- Relatively high operating temperatures, and reasonable magnetoresistance makes the CrN/P/CrN system an appealing candidate for a lateral spin-valve device. [25]

CONTACT PERSON

Aybey MOGULKOC

mogulkoc@science.ankara.edu.tr

REFERENCES

[1] J. Meng, J.-J. Chen, Y. Yan, D.-P. Yu, and Z.-M. Liao, Nanoscale 5, 8894 (2013).
[2] G. Li, S. Sun, et al., Sens. Actuator A-Phys. 126, 98 (2006).
[3] W. Qiu, et al., Sens. Actuator A-Phys. 265, 174 (2017).
[4] I. Zutic, J. Fabian, and S. Das Sarma, Rev. Mod. Phys. 76, 323 (2004).
[5] W. Han, R. K. Kawakami, M. Gmitra, and J. Fabian, Nat. Nanotech. 9, 794 (2014).
[6] Z. Xiong, D. Wu, Z. V. Vardeny, and J. Shi, Nature 427, 821 (2004).
[7] S. Ikeda,, et al., Appl. Phys. Lett. 93, 082508 (2008).
[8] E. W. Hill, A. K. Geim, K. Novoselov, F. Schedin, and P. Blake, IEEE Trans. Magn. 42, 2694 (2006).
[9] S. Cho, Y.-F. Chen, and M. S. Fuhrer, Appl. Phys. Lett. 91, 123105 (2007).
[10] M. Z. Iqbal, , et al., Nano Res. 6, 373 (2013)
[11] S. Entani, H. Naramoto, and S. Sakai, J. Appl. Phys. 117, 17A334 (2015).
[12] B. Huang, et al., Nature 546, 270 (2017).
[13] S. Jiang, L. Li, Z. Wang, K. F. Mak, and J. Shan, Nat. Nanotech. 13, 549 (2018).
[14] G. Kresse and D. Joubert, Phys. Rev. B 59, 1758 (1999).
[15] G. Kresse and J. Furthmüller, Comp. Mat. Sci. 6, 1550 (1996).
[16] G. Kresse and J. Furthmüller, Phys. Rev. B 54, 11169 (1996).
[17] J. P. Perdew, K. Burke, and M. Ernzerhof, Phys. Rev. Lett. 77, 3865 (1996).
[18] V. I. Anisimov, F. Aryasetiawan, and A. I. Lichtenstein, J. Phys.: Cond. Matter 9, 767 (1997).
[19] S. L. Dudarev, et al.,, Phys. Rev. B 57, 1505 (1998).
[20] G. Pizzi, D. Volja, B. Kozinsky, M. Fornari, and N. Marzari, Comp. Phys. Commun. 185, 8. 422 (2014).
[21] A. A. Mostofi, et al.,, Comp. Phys. Commun. 178, 685 (2008).
[22] N. Marzari and D. Vanderbilt, Phys. Rev. B 56, 12847 (1997).
[23] N. Marzari, A. A. Mostofi, J. R. Yates, I. Souza, and D. Vanderbilt, Rev. Mod. Phys. 84, 1419 (2012).
[24] J. Rusz, I. Turek, and M. Divis, Phys. Rev. B 71, 174408 (2005).
[25] M. Modarresi, A. Mogulkoc, Y. Mogulkoc and A.N. Rudenko, Phys. Rev. Applied 11, 064015 (2019).

Graphene Industrial Forum &2DM 2020